Journal of Experimental Botany, Vol. 63, No. 16, pp. 5919–5933, 2012
doi:10.1093/jxb/ers244

Journal of Experimental Botany
www.jxb.oxfordjournals.org

RESEARCH PAPER

Co-evolution between *Grapevine rupestris stem pitting-associated virus* and *Vitis vinifera* L. leads to decreased defence responses and increased transcription of genes related to photosynthesis

Giorgio Gambino[1,*], Danila Cuozzo[2], Marianna Fasoli[3], Chiara Pagliarani[2], Marco Vitali[2], Paolo Boccacci[1], Mario Pezzotti[3] and Franco Mannini[1]

[1] Plant Virology Institute, National Research Council (IVV-CNR), UOS Grugliasco, Via L. da Vinci 44, 10095 Grugliasco-TO, Italy
[2] Department of Arboriculture and Pomology, University of Torino, Via L. da Vinci 44, 10095 Grugliasco-TO, Italy
[3] Department of Biotechnology, University of Verona, Strada le Grazie 15, 37134 Verona, Italy

* To whom correspondence should be addressed. E-mail: g.gambino@ivv.cnr.it

Received 6 July 2012; Revised 2 August 2012; Accepted 3 August 2012

Abstract

Grapevine rupestris stem pitting-associated virus **(GRSPaV) is a widespread virus infecting *Vitis* spp. Although it has established a compatible viral interaction in *Vitis vinifera* without the development of phenotypic alterations, it can occur as distinct variants that show different symptoms in diverse *Vitis* species. The changes induced by GRSPaV in *V. vinifera* cv 'Bosco', an Italian white grape variety, were investigated by combining agronomic, physiological, and molecular approaches, in order to provide comprehensive information about the global effects of GRSPaV. In two years, this virus caused a moderate decrease in physiological efficiency, yield performance, and sugar content in berries associated with several transcriptomic alterations. Transcript profiles were analysed by a microarray technique in petiole, leaf, and berry samples collected at véraison and by real-time RT-PCR in a time course carried out at five grapevine developmental stages. Global gene expression analyses showed that transcriptomic changes were highly variable among the different organs and the different phenological phases. GRSPaV triggers some unique responses in the grapevine at véraison, never reported before for other plant–virus interactions. These responses include an increase in transcripts involved in photosynthesis and CO_2 fixation, a moderate reduction in the photosynthesis rate and some defence mechanisms, and an overlap with responses to water and salinity stresses. It is hypothesized that the long co-existence of grapevine and GRSPaV has resulted in the evolution of a form of mutual adaptation between the virus and its host. This study contributes to elucidating alternative mechanisms used by infected plants to contend with viruses.**

Key words: Abiotic stresses, GRSPaV concentrations, Nimblegen arrays, qRT-PCR, resistance genes, Rubisco activase.

Introduction

Grapevine rupestris stem pitting-associated virus (GRSPaV) is a member of the genus *Foveavirus*, family Betaflexiviridae, associated with rupestris stem pitting (RSP), a disorder of the rugose wood (RW) complex (Martelli, 1993). In grapevine (*Vitis* spp.), RW is a widespread viral disease complex, characterized by alterations in the plant woody cylinder, and distinguished as four different syndromes, which can be identified by graft inoculation to indicator vines: RSP, Kober stem grooving, LN33 stem grooving, and corky bark (Martelli, 1993). RSP is characterized by pitting symptoms on the woody cylinder below the graft union on the *Vitis rupestris* cv. St George indicator. GRSPaV is usually found in *Vitis vinifera* L. cultivars in a latent state; several distinct variants have

often been identified in infected grapevine scions, while a single variant with more sequence homogeneity has been detected in rootstock varieties (Meng *et al*., 2006). This could be the result either of separate introductions of different GRSPaV variants in the same *V. vinifera* plant through grafting with different propagating materials from distant viticultural areas or of natural viral genome mutations. Meng *et al*. (2006) suggested a nomenclature for grouping GRSPaV variants into four lineages: GRSPaV-1, GRSPaV-SG1, GRSPaV-BS, and GRSPaV-VS, based on the presence of a specific reference isolate within each group, and characterized by different symptoms on the indicators. Infection with strain GRSPaV-SG1 is asymptomatic; strain GRSPaV-1 causes only mild symptoms in *V. rupestris* (Meng *et al*., 2005). In addition, some GRSPaV strains are shown to have a close association with vein necrosis in 110 Richter (*V. rupestris*×*V. berlandieri*) (Bouyahia *et al*., 2005) and Syrah decline (Lima *et al*., 2006), even though their role in the latter disease is yet to be resolved (Goszczynski, 2010).

GRSPaV is the most prevalent among grapevine viruses, and can be spread via vegetative propagation, grafting, and possibly through seeds, but no biological vectors have been reported (Meng and Gonsalves, 2003). Moreover, it is particularly difficult to eliminate GRSPaV by traditional sanitation techniques (i.e. meristem tip culture and thermotherapy) (Gribaudo *et al*., 2006) and, accordingly, it is often associated with other viral entities.

In plants, a systemic viral infection (also for compatible interactions) always relies on complex molecular interactions between the invading virus and the host plant, where the virus recruits several host proteins and metabolites for the translation and replication of its genome (Whitham *et al*., 2003). Over the years, many authors have analysed global gene expression changes in several plant–virus interactions (Whitham *et al*., 2003; Babu *et al*., 2008; Baebler *et al*., 2009). However, these studies were principally concerned with viruses infecting herbaceous species with a clear symptomatology in the host. Plant–virus interactions in woody perennial plants, such as grapevine, in some cases showed more complex transcriptomic responses on the basis of the different biology and the long life cycle of the host (Espinoza *et al*., 2007*a*; Vega *et al*., 2011). To date, the molecular interactions between GRSPaV and grapevine are largely unknown, and little has been reported on the agronomic effects of this virus. Reynolds *et al*. (1997) described a few or no negative impacts on yield components in GRSPaV-infected plants; however, the health status of the grapevines analysed in this work was not clear. In subsequent reports, GRSPaV was always associated with other viruses that cause symptomatic infections (Komar *et al*., 2010).

In this communication, the results obtained by applying global gene expression analyses combined with physiological and agronomic studies in grapevine infected by GRSPaV, in order to identify the molecular and physiological changes triggering the host response to this virus, are discussed. This study shows the existence in grapevine of some original responses against this widespread virus, never reported before for other plant–virus interactions.

Materials and methods

Plant material

The study was carried out in a vineyard planted in 2002 in Albenga (Liguria), North-West Italy, where a row was established with the white grape cultivar 'Bosco' (*V. vinifera* L.). Vines were grafted onto 1103 P rootstock, spaced 2.10 m between rows and 1.00 m between plants for a total plant density of ~4700 vines ha^{-1}. Vines were vertically trained and one-cane pruned (Guyot), leaving 12 buds per vine.

All 'Bosco' plants were derived by vegetative propagation from a single mother plant originally infected by *Grapevine virus A* (GVA), *Grapevine leafroll-associated virus-1* (GLRaV-1), *Grapevine leafroll-associated virus-3* (GLRaV-3), and GRSPaV, and further subjected to sanitation. The *in vitro* thermotherapy and meristem tip culture sanitation techniques successfully eliminated most of the viruses present in the mother vine, but they did not provide satisfactory results in the eradication of GRSPaV, leaving some lines still infected by the virus.

The sanitary status of all 'Bosco' plants in the vineyard was tested in 2010 by multiplex RT-PCR (Gambino and Gribaudo, 2006) to detect nine viruses that commonly infect grapevine in Italy and in other viticultural countries: *Arabis mosaic virus* (ArMV), *Grapevine fanleaf virus* (GFLV), *Grapevine virus B* (GVB), *Grapevine fleck virus* (GFkV), GLRaV-1, GLRaV-2, GLRaV-3, GVA, and GRSPaV. The multiplex RT-PCR analyses were repeated in 2011 to confirm the sanitary status of the plants selected for the trial.

Physiological and agronomical parameters

Twelve vines in the same row, six GRSPaV-free and six GRSPaV-infected (two replicates of three plants each), were selected in order to carry out experimental observations during the growing season in 2010 and 2011. Eco-physiological parameters were registered in different phenological phases according to the E-L System modified by Coombe (1995): berry setting (E-L27), pea sized berries (E-L31), véraison (E-L35), and harvest (E-L38). During summer 2010, the main physiological parameters, namely photosynthetic rate (P_n), transpiration rate (E), stomatal conductance (g_s), and substomatal CO_2 concentration (c_i), were monitored by a portable infra-red gas analyser ADC-LCpro+ system (ADC Bioscientific Ltd, Hoddesdon, UK), whereas leaf chlorophyll content was measured using a non-destructive portable chlorophyll meter SPAD-502 (Konica Minolta, Tokyo, Japan). Physiological data were registered from 12 am to 4 pm on six leaves (three basal and three apical) per plant in E-L31 (31 July 2010) and E-L35 (20 August 2010) phases. These physiological measurements were repeated in 2011 on the same vines, but data were collected at four stages: E-L27 (14 June 2011), E-L31 (14 July 2011), E-L35 (2 August 2011), and E-L38 (25 August 2011).

During the 2010 and 2011 vegetative growth periods, some relevant agronomic parameters were determined for each vine: bud burst index (Eynard *et al*., 1978) and shoot fertility (number of inflorescences/shoot) in the spring, and yield, number of bunches, as well as the average weight, length, and width of both bunches and berries at harvest. Average bunch data were derived by counting and weighing all the harvested bunches, while biometric berry data were measured on a sample of 120 berries for plants of each sanitary status. The grapes of every single vine were separately crushed and, on the obtained must, the main ripening parameters (total soluble solids, °Brix; titratable acidity, g l^{-1}; and pH) were measured according to the methods of the International Organization of Vine and Wine (http://www.oiv.int/oiv/info/frmethodesinternationalesvin). Physiological and agronomic data collected over these two years were statistically analysed by applying the analysis of variance (ANOVA) *F*-test.

Microarray experiment and data analysis

Microarray analysis was carried out on RNA extracted from leaves, petioles, and berries collected at véraison (E-L35) in 2010. From each of the six GRSPaV-free and six GRSPaV-infected vines selected for the evaluation of physiological and agronomic parameters, six leaves (three basal and three apical) with petioles and 12 berries from three different bunches were collected. Samples from each organ were arbitrarily pooled into three independent biological replicates and total RNA was extracted according to the method described by Gambino *et al*. (2008).

RNA quality and quantity were determined using both the Nanodrop (Nanodrop 2000, Thermo Scientific, Wilmington, DE, USA) and the Bioanalyzer (2100 Bioanalyzer, Agilent, Santa Clara, CA, USA) instruments. cDNA synthesis, labelling, hybridization, and washing were performed according to the NimbleGen Arrays User's Guide (V 3.2). Each hybridization was carried out on a NimbleGen microarray 090818 Vitis exp HX12 (Roche, NimbleGen Inc., Madison, WI, USA), representing 29 549 predicted genes on the basis of the 12X grapevine V1 gene prediction version (http://srs.ebi.ac.uk/). The chip probe design is available at: http://ddlab.sci.univr.it/FunctionalGenomics/.

Microarray chips were scanned using the Axon GenePix 4400 A scanner at 532 nm (Cy-3 absorption peak) and GenePix Pro7 software (Molecular Devices, Sunnyvale, CA, USA), according to the manufacturers' instructions. Images were elaborated using the NimbleScan v2.5 software (Roche), which produces Pair Files containing raw signal intensity data for each probe and Calls Files with normalized expression data derived from the average of the intensities of the four probes for each gene. All microarray expression data are available at GEO under the series entry GSE36632.

A Pearson correlation analysis was carried out to evaluate the robustness of the three biological replicates for each sample (R software). A significance analysis of microarray (SAM; Tusher *et al*., 2001) was implemented using the TMeV software (http://www.tm4.org/mev), with a false discovery rate (FDR) of 1%. Differentially expressed genes were selected for each comparison among those contemporarily significant at the 'between-subjects' *t*-test and at the fold change threshold applied. Three separate tests were then conducted among each sample group (leaf, petiole, and berry) against its own control (by the TMeV software), setting a *P*-value based on the t-distribution and without correction (P-value < 0.01). For all experiments, the corresponding gene expression data were pre-evaluated, in order to assess the prerequisite of normal distribution (R software). Annotations of significant differentially expressed probes were checked and updated by a query of the corresponding nucleotide sequence retrieved from the 12X grapevine V1 gene prediction database (http://srs.ebi.ac.uk/) against the UniProt/TrEMBL protein database (Viridiplantae match), applying the blastx algorithm with a minimum significance value (e-value) of $1e^{-10}$ and using the software Blast2GO v.2.5.0 (www.blast2go.org/). For each organ, probes were functionally annotated following the Gene Ontology (GO) classification (www.geneontology.org), using the GO mapping step of Blast2GO software. GO terms of differentially expressed probes were thus grouped into higher order functional categories. The homogeneity of frequencies of hits falling in the functional categories was tested using a χ^2 test.

Real-time RT-PCR

Validation of microarray data was carried out in biological triplicates on the same RNA samples subjected to microarray analysis. Primers (Supplementary Table S1 available at *JXB* online) were designed by the Primer Express® 3.0 software (Applied Biosystems, Foster City, CA, USA) and qRT-PCRs were performed using the PowerSYBR Green master mix (Applied Biosystems), as previously described (Gambino *et al*., 2011). Four endogenous housekeeping genes, actin (*Act*), ubiquitin (*Ubi*) (Gambino *et al*., 2011), glyceraldehyde-3-phosphate-dehydrogenase (*GAPDH*), and elongation factor 1-α (*EF1-α*) (Reid *et al*., 2006), were considered for use in qRT-PCR after analysis of gene expression stability in the geNorm software (Vandesompele *et al*., 2002; http://medgen.ugent.be/~jvdesomp/genorm/). The geometric mean of the expression ratios of the two most stable housekeeping genes were used as the normalization factor for all samples. Specific annealing of primers was controlled on dissociation kinetics performed at the end of each qRT-PCR run. Gene expression was determined as the mean, and standard errors were calculated over all biological and technical replicates.

Molecular responses of 26 selected genes were analysed in GRSPaV-infected grapevines in 2011. qRT-PCR was carried out on berries taken from the same four phenological phases considered for physiological measurements, while for leaves and petioles, in addition to these phases, a precocious stage was included, where inflorescences were well developed with single separated flowers (E-L17; 11 May 2011) (Coombe, 1995).

Relative quantification of GRSPaV genomes was carried out on each organ for all the phenological phases using primers designed on viral RNA-dependent RNA polymerases (RdRps) to exclude the amplification of subgenomic mRNAs (Supplementary Table S1 at *JXB* online) and following the same qRT-PCR parameters reported above.

Results

GRSPaV concentration in infected grapevines

During the preliminary phase of the work, both grapevines infected by GRSPaV (but negative for other viruses) and plants negative for nine viruses commonly infecting grapevine were identified by multiplex RT-PCR. GRSPaV concentrations in leaf and petiole were roughly similar during 2011, although the virus was more concentrated in petioles at the beginning of the season (E-L17, 11 May 2011) (Fig. 1). Surprisingly, in all the samples collected in 2011, the highest levels of viral RNA were detected in berries and, in particular, in young berries (E-L27, 14 June 2011). Although the differences between the organs were maintained between the two years (viral RNA was always more concentrated in the berry), at véraison 2010, the virus was ~10 times more concentrated than at each stage analysed in 2011 (Fig. 1).

Physiological and agronomic performance of GRSPaV-infected grapevines

In 2010, chlorophyll content (Fig. 2A) and P_n (Fig. 2B) were significantly lower in GRSPaV-infected plants at the end of the season. As expected, c_i (Fig. 2C) was higher at the E-L31 stage (31 July 2010) and was related to a decrease in P_n rates. In 2011, the trend of physiological responses was similar to that observed the previous year; statistically significant differences were found

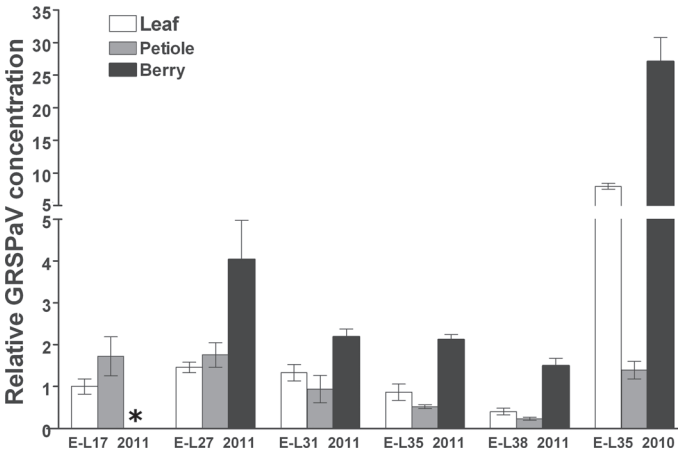

Fig. 1. Quantification of GRSPaV RNA in leaf, petiole, and berry samples from cv 'Bosco' as determined by qRT-PCR. Samples were collected at véraison in 2010 (E-L35) and at five developmental stages in 2011 (E-L17, -27, -31, -35, and -38). qRT-PCR signals were normalized to *Act* and *UBI* transcripts. Data are presented as the mean± SE of biological and technical replicates. *Berries not present at this stage.

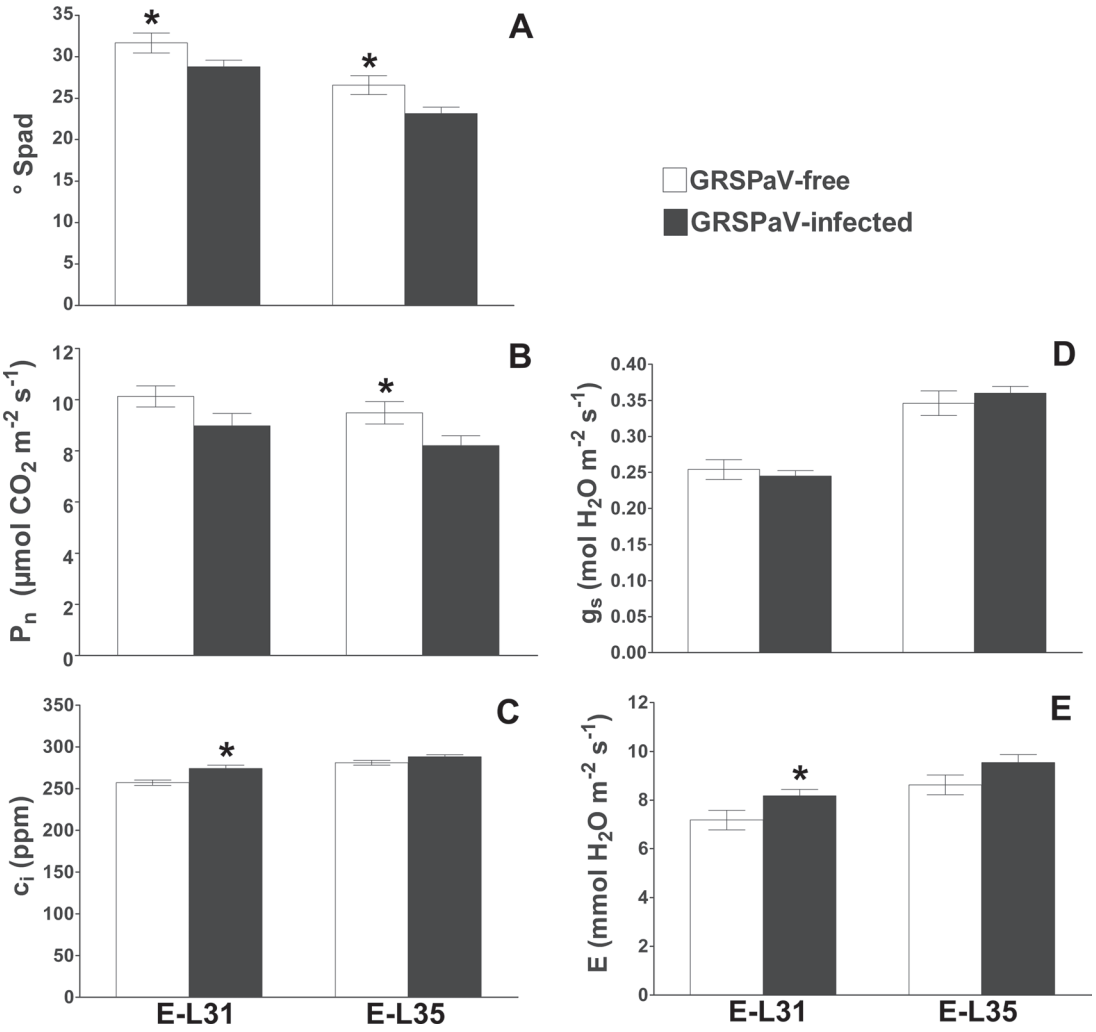

Fig. 2. Changes in: (A) chlorophyll content (Spad), (B) net photosynthesis (P_n), (C) intercellular CO_2 concentration (c_i), (D) stomatal conductance (g_s), and (E) transpiration (E) in GRSPaV-free (white columns) and GRSPaV-infected (black columns) grapevine leaves. Measurements (n=36) were taken during two phenological periods: pea sized berries (E-L31) and véraison (E-L35) 2010. Bars are the standard error of the mean. Asterisks show significant differences between infected and GRSPaV-free leaves ($P < 0.05$).

only in some cases. In infected plants, gas exchange measurements confirmed the negative effect of the virus on P_n rates at harvest (E-L38, 25 August 2011) (Supplementary Fig. S1B at *JXB* online); g_s (Supplementary Fig. S1D) and E (Supplementary Fig. S1E) values increased in GRSPaV-free grapevines, whereas leaf chlorophyll content was very similar between the GRSPaV-infected and GRSPaV-free plants (Supplementary Fig. S1A).

In terms of agronomic and qualitative traits, the results collected during the two vintages showed similar trends (Table 1). In particular, yield was favoured in uninfected plants, although only the 2010 data were statistically significant. In 2011, differences in both yield and sugar content were less evident; however, the effect of virus infection in reducing the dimension of bunches and berries was clearly confirmed.

Microarray analysis

A comparative microarray analysis was carried out on infected and GRSPaV-free samples collected at véraison in 2010. A multiclass comparison analysis was first performed by applying SAM with an FDR of 1%: 24 902 genes modulated were identified in at least one comparison. Three independent *t*-tests were carried out for each organ to identify among these genes the expression profiles with the greatest contribution to specific tissue responses. Thus 877 genes were found in leaf, 596 in petiole, and 233 in berry, showing significant expression changes in GRSPaV-infected grapevines compared with their respective control (Fig. 3; Supplementary Table S2 at *JXB* online).

Differentially expressed transcripts were grouped in 11 functional classes, on the basis of the specific biological process in which they were involved, by following the GO classification. In response to GRSPaV, the modulation of gene expression was highly variable between petioles, leaves, and berries (Fig. 4), and no modulated transcripts were shared among the three organs (Fig. 3).

Global gene expression changes in GRSPaV-infected petioles

In petioles, GRSPaV induced a general up-regulation of genes involved in the cytoskeleton structure, such as microtubules and

Table 1. *Field performances of GRSPaV-infected and uninfected grapevines of 'Bosco' in two consecutive years*

Data	2010			2011		
	GRSPaV-free	GRSPaV-infected	*P*-value	GRSPaV-free	GRSPaV-infected	*P*-value
Bud burst index	4.37±0.29	4.52±0.18	NS	3.6±0.24	3.77±0.21	NS
Fertility (n°. inf/shoot)	0.49±0.10	0.62±0.13	NS	0.88±0.15	1.03±0.16	NS
Yield (kg/vine)	2.80±0.34	1.92±0.13	*	2.75±0.44	2.46±0.81	NS
Bunch/vine (n°.)	12±0.7	10±0. 7	NS	8±0.8	8±2.1	NS
Bunch weight (g)	250±24.3	191±15.0	NS	333±28.3	290±18.4	NS
Bunch length (cm)	21.3±0. 6	19.4±0.6	*	19.0±0.7	19.0±0.6	NS
Bunch width (cm)	11.7±0.5	9.5±0.5	***	11.0±0.5	10.0±0.4	*
Peduncle length (cm)	4.5±0.3	4.2±0.3	NS	7.0±0.3	6.0±0.3	NS
Berry weight (g)	2.64±0.41	2.34±0.5	***	2.8±0.86	2.3±0.69	***
Berry length (cm)	1.7±0.02	1.6±0.02	***	1.6±0.01	1.4±0.01	***
Berry width (cm)	1.6±0.02	1.4±0.01	***	1.6±0.01	1.4±0.01	***
Total soluble solids (°Brix)	22.22±0.26	21.10±0.42	*	23.18±1.02	22.98±0.95	NS
Titratable acidity (g l^{-1})	2.89±0.08	3.4±0.15	*	6.27±0.62	6.66±0.41	NS
pH	3.27±0.03	3.38±0.03	NS	3.01±0.07	3.09±0.03	NS

All data are expressed as average values ±SE.
*$P \leq 0.05$; **$P \leq 0.01$; ***$P \leq 0.001$; NS, not significant.

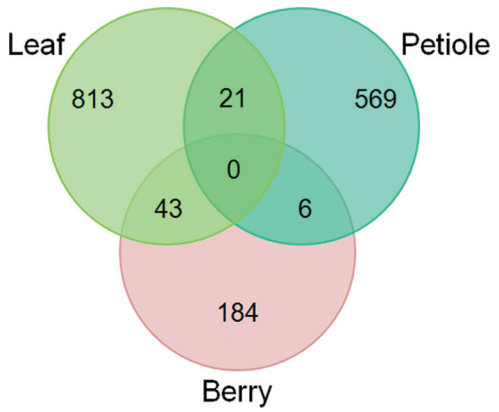

Fig. 3. Venn diagrams of the number of transcripts showing significantly different abundance ($P < 0.01$) between GRSPaV-free and infected grapevines in three different organs at véraison in 2010.

microfilaments. Interestingly, a gene encoding cyclin delta-3 (*CYCD3;1*, VIT_18s0001g09920), which mainly drives the transition from G_1 to S phase in the cell cycle, was down-regulated. An overall up-regulation of transcripts linked to nucleic acid metabolism, regulation of transcription, and several genes encoding methyl-CpG-binding domain-containing proteins (*MBD*, VIT_07s0104g00770) and histone deacetylases (*HDAC*, VIT_07s0141g00150) was also found (Table 2; Supplementary Table S2 at *JXB* online).

Carbohydrate metabolism was modified through the up-regulation of some genes linked to glycolysis and, in parallel, through a decrease in the pentose phosphate pathway. Only a few genes involved in defence response were modulated, and some of them (enhanced disease resistance, NBS class of disease resistance proteins) were down-regulated. However, several transcripts involved in stress [heat shock proteins (*HSP*), reactive oxygen species (ROS)], senescence [senescence-associated gene 101 (*SAG101*, VIT_14s0066g01810)], transport, signal transduction, and hormone metabolism were up-regulated (Supplementary Table S2 at *JXB* online).

A general activation of genes responsible for the transport of molecules across cell membranes, and signal transduction processes (Ser/Thr protein kinases) was observed. Hormone metabolism was also altered, with an increase in ethylene gene transcription [1-aminocyclopropane-1-carboxylate oxidase (*ACO*, VIT_00s2086g00010)] and a repression of genes linked to the auxin pathway. Among the transcripts involved in secondary metabolism, several genes linked to terpenoid and phenylpropanoid biosynthesis were positively modulated (Table 2; Supplementary Table S2 at *JXB* online).

Global gene expression changes in GRSPaV-infected leaves

In leaves, responses to GRSPaV infection dramatically changed in comparison with the metabolic reactions observed in petioles, since a general down-regulation of the main functional gene categories was also observed (Fig. 4).

The up-regulation of transcripts coding for the senescence-inducible chloroplast stay-green protein 2 (*SGR2*, VIT_18s0001g01210), of the ribulose bisphosphate carboxylase/oxygenase activase (*Rubisco activase*, VIT_13s0019g02050), and of several chloroplastic isoforms of genes tied to the Calvin cycle: fructose 1,6-bisphosphatase (*FBPase*, VIT_08s0007g01570), glyceraldehyde-3-phosphate dehydrogenase (*GAPDH chl*, VIT_14s0068g00680), and fructose-bisphosphate aldolase (*FBA*, VIT_03s0038g00670) was observed (Table 2).

Moreover, within the Calvin cycle, the expression of genes involved in glycolysis, in the pentose phosphate pathway, and in the tricarboxylic acid (TCA) cycle was negatively modulated (Supplementary Table S2 at *JXB* online). Starch metabolism was positively influenced through an increase in starch synthase transcription (VIT_02s0025g02790).

Table 2. *Selection of genes significantly modulated in GRSPaV-infected petioles, leaves, and berries at véraison in 2010, classified on the base of the GO category of biological process*

Gene ID refers to NimbleGen microarray 090818 Vitis exp HX12. For each gene the best UniProt match with the related annotation and the expression ratio value (fold change) are reported.

Sequence ID (Genoscope 12X V1)	UniProt match and annotation	Fold change		
		Petiole	Leaf	Berry
Photosynthesis and energy metabolism				
VIT_01s0010g00920	(P08927) Rubisco large subunit-binding protein, chloroplastic		1.38	
VIT_04s0023g00410	(Q41385) Photosystem I reaction centre subunit chloroplastic	1.27		1.33
VIT_07s0005g04400	(Q0JG75) Photosystem II reaction centre psb28, chloroplastic		1.75	
VIT_10s0003g02900	(P27495) Chlorophyll *a-b*-binding protein, chloroplastic (LHCI type I CAB-40)		1.46	
VIT_13s0019g02050	(Q40281) Ribulose bisphosphate carboxylase oxygenase, chloroplastic		1.47	
VIT_18s0001g01210	(A7NY33) Senescence-inducible chloroplast stay-green protein 2 (SGR superfamily)		1.63	
VIT_19s0014g00160	(P12333) Chlorophyll *a-b*-binding, chloroplastic (LHCII type I CAB-1)		2.22	
Carbohydrate metabolism				
VIT_00s0304g00080	(A7R008) Trehalose-6-phosphate phosphatase		1.89	–1.32
VIT_01s0010g02460	(P25858) Glyceraldehyde-3-phosphate dehydrogenase cytosolic		–2.23	
VIT_02s0025g02790	(O82627) Starch synthase		1.34	
VIT_03s0038g00670	(Q9SJU4) Fructose-bisphosphate aldolase chloroplastic		1.47	
VIT_04s0044g01120	(P25141) Alcohol dehydrogenase		–3.02	
VIT_05s0077g00280	(Q9LIR6) Beta-amylase chloroplastic			1.14
VIT_07s0005g02800	(P55230) ADP-glucose pyrophosphorylase		–1.41	
VIT_08s0007g01570	(P46275) Fructose 1–6 biphosphatase		1.19	
VIT_12s0057g01030	(O24357) Glucose-6-phosphate 1-dehydrogenase, chloroplastic	–1.35		
VIT_12s0134g00160	(Q8LDW9) Xyloglucan endotransglucosylase hydrolase protein 9		2.4	
VIT_14s0068g00680	(P12858) Glyceraldehyde-3-phosphate dehydrogenase chloroplastic		1.29	
VIT_14s0108g00540	(Q8VYN6) Phosphofructokinase chloroplastic			–1.19
VIT_15s0046g01000	(CAN67648) Trehalose-6-phosphate phosphatase	–1.20		
VIT_15s0046g03520	(Q1W376) Phosphomannomutase	1.40	1.44	
VIT_19s0090g00920	(Q01401) 1,4-Alpha-glucan-branching enzyme	1.70		
Nucleic acid metabolism and transcriptional regulation				
VIT_00s0187g00350	(Q9SU25) Transcription initiation factor IIF subunit alpha	1.16		
VIT_02s0033g00450	(C0LA45) Transcription factor mybA3			1.36
VIT_06s0004g07100	(D7SJS8) Eukaryotic translation initiation factor 2 alpha subunit	1.27		
VIT_07s0104g00770	(Q9LYB9) Methyl-binding domain-containing protein 4	1.46		
VIT_07s0141g00150	(Q338B9) Histone acetyltransferase gcn5		–1.38	
VIT_12s0134g00100	(P29766) 60s Ribosomal protein l8			1.10
VIT_12s0134g00480	(Q7XBH4) Myb-related protein myb4		2.63	
VIT_14s0068g01770	(Q9FYA2) Wrky transcription factor 75		–2.09	
VIT_15s0024g00350	(F6I5H6) BTAF1 RNA polymerase II, B-TFIID transcription factor-associated	1.67		
VIT_15s0046g00170	(A4F4L3) Transcription factor mybPA1			1.54
VIT_15s0046g00320	(Q9LNJ5) Basic helix–loop–helix protein 13		1.43	
VIT_15s0048g02380	(Q9SP32) Endoribonuclease dicer homologue 1		1.32	
Secondary metabolism				
VIT_00s0271g00030	(P0CV94) Nerolidol synthase 1		3.59	
VIT_00s0389g00040	(Q05047) Secologanin synthase	3.35		
VIT_04s0008g01860	(Q05047) Secologanin synthase		–1.32	–1.62
VIT_05s0136g00260	(P48387) Chalcone synthase			1.48
VIT_06s0009g02920	(P48419) Flavonoid 3-hydroxylase 2	–1.63		
VIT_10s0042g00850	(P51070) Stilbene synthase 2	2.10		
VIT_11s0052g01600	(P51094) Anthocyanidin 3-*O*-glucosyltransferase			–1.19
VIT_12s0134g00030	(Q7XAS7) Isoprene synthase, chloroplastic precursor			–4.32
VIT_12s0134g00030	(Q7XAS7) Isoprene synthase, chloroplastic		–1.29	
VIT_13s0106g00790	(Q0ZIW8) Mevalonate diphosphate decarboxylase			–1.12
VIT_14s0128g00330	(P46086) Mevalonate kinase	1.61		
VIT_16s0039g01300	(P45730) Phenylalanine ammonia-lyase		–1.33	
VIT_16s0100g01130	(P28343) Stilbene synthase 1		–1.86	
VIT_17s0000g01790	(Q84P23) 4-Coumarate-ligase-like 9			–1.28
VIT_18s0001g03470	(Q9ZWQ9) Flavonol synthase flavanone 3-hydroxylase		2.55	–3.12

Table 2. *Continued*

Sequence ID (Genoscope 12X V1)	UniProt match and annotation	Fold change		
		Petiole	Leaf	Berry
Response to hormone stimulus and hormone biosynthesis				
VIT_16s0013g00980	(Q40478) Ethylene-responsive transcription factor	1,56		
VIT_00s2086g00010	(P31237) 1-Aminocyclopropane-1-carboxylate oxidase (ACO)	1.47	–1.16	
VIT_02s0087g00930	(O49675) 9-*cis*-Epoxycarotenoid dioxygenase (NCED)		1.66	
VIT_04s0023g00320	(Q9FFD0) Auxin efflux carrier component 8	–1.83	1.33	
VIT_05s0049g00260	(Q84MB3) 1-Aminocyclopropane-1-carboxylate oxidase homologue 1		–1.58	
VIT_07s0031g00710	(Q9SZ06) Ethylene-responsive transcription factor erf109		2.45	
VIT_11s0016g02380	(Q9ZUN4) 1-Aminocyclopropane-1-carboxylate oxidase (ACO)			–1.16
VIT_18s0001g01390	(Q0JH50) Gibberellin 20 oxidase 2		1.85	
VIT_18s0001g03180	(Q6J163) Auxin-induced protein 5ng4	–1.73		
VIT_18s0041g02270	(B9FSC8) 12-Oxophytodienoate reductase 11		1.64	–1.50
VIT_18s0072g00260	(Q70II3) Ethylene-responsive transcription factor erf110			–1.72
Response to endogenous stimulus and signal transduction				
VIT_00s0125g00210	(C0LGH3) Probable lrr receptor-like serine threonine-protein kinase	1.73	–1.45	
VIT_00s1830g00010	(Q3ECH2) Receptor-like protein kinase			–1.58
VIT_04s0008g03530	(Q9C7A2) Ankyrin repeat-containing protein		–2.54	
VIT_06s0004g07920	(Q9LVL5) Serine threonine-protein kinase		–1.49	
VIT_08s0040g01250	(Q10KY3) Calcium calmodulin-dependent serine threonine-protein kinase 1	1.55		
VIT_09s0002g03100	(C0LGD9) Probable LRR receptor-like serine threonine-protein kinase		–2.06	
VIT_09s0002g04560	(D7U0K2) Calmodulin-binding protein			–1.35
VIT_13s0158g00150	(Q9SV05) Serine threonine-protein kinase-like protein	1.28		
VIT_17s0000g04490	(Q9FN48) Calcium sensing chloroplastic		1.73	
Response to disease and abiotic stress				
VIT_00s0317g00040	(A9UFY0) Dehydroascorbate reductase	1.46		
VIT_00s0317g00050	(Q9FRL8) Dehydroascorbate reductase		1.30	
VIT_00s0357g00080	(A7PQW3) β1–3 Glucanase		–2.39	
VIT_01s0010g00680	(P51819) Heat shock protein 83	1.63		
VIT_01s0011g01900	(Q8H121) Glutathione *S*-transferase C-terminal			1.12
VIT_02s0025g00280	(P51819) Heat shock protein 83			–1.48
VIT_02s0025g04270	(P81370) Thaumatin-like protein		–5.29	–1.46
VIT_03s0088g00700	(P11670) Pathogenesis-related protein 1		–1.98	–1.78
VIT_04s0008g01520	(P05477) 21 kDa class II heat shock protein			–2.81
VIT_04s0008g07260	(F6H3L6) EDR2 (enhanced disease resistance 2)	–1.49		
VIT_05s0020g02120	(Q9ZV04) Peroxidase	–1.58		
VIT_05s0051g00240	(Q03664) Glutathione *S*-transferase	1.69		
VIT_05s0077g01150	(P52407) β1–3 Glucanase		–1.35	–2.53
VIT_05s0094g00340	(O04138) Pathogenesis-related-3 chitinase 4		–1.37	
VIT_06s0004g05680	(P32110) Glutathione *S*-transferase	1.48		
VIT_06s0004g07770	(A7NY33) Peroxidase			–1.26
VIT_08s0007g01420	(Q03662) Glutathione *S*-transferase		1.28	
VIT_08s0007g06040	(Q03773) β1–3 Glucanase			–1.31
VIT_08s0007g06060	(P52408) β1–3 Glucanase		–3.97	–2.39
VIT_10s0042g01180	(Q9SHF3) Protein argonaute 2 (AGO2)			1.16
VIT_14s0108g01070	(Q9FLJ2) NAC domain-containing protein 100		1.53	
VIT_16s0050g02230	(P51614) Acidic endochitinase		–1.74	
VIT_17s0000g07190	(P42730) Heat shock protein 101		–2.45	
VIT_17s0000g07400	(F6GSY6) Disease resistance protein (EDS1)		–1.78	
VIT_18s0072g00160	(Q96520) Peroxidase		–1.49	
VIT_18s0122g01320	(P17598) Catalase 3		1.36	
Transport				
VIT_00s0625g00020	(Q8RXN0) ABC transporter G family member 11	3.96		
VIT_01s0011g00600	(P11869) Triose phosphate phosphate transporter, chloroplastic s		2.13	
VIT_02s0087g00580	(Q9LVE0) Nitrate transporter		1.33	
VIT_05s0020g03140	(Q94AZ2) Hexose transporter protein HT3			–2.27
VIT_06s0004g00610	(Q9FYC2) Accelerated cell death 1 (ACD1)	1.43	1.79	

Table 2. *Continued*

Sequence ID (Genoscope 12X V1)	UniProt match and annotation	Fold change		
		Petiole	Leaf	Berry
VIT_10s0116g00760	(Q94B38) Glucose-6-phosphate phosphate translocator, chloroplastic		–1.35	
VIT_11s0016g05170	(Q9SZY4) Nitrate transporter	1.82		
VIT_11s0149g00050	(O04249) Hexose transporter protein HT5			1.13
VIT_16s0050g02480	(Q9LYS2) ABC transporter C family member 10		1.57	
Cell cycle, morphogenesis, and homeostasis				
VIT_00s0194g00260	(Q8GYX3) Microtubule-associated protein 70–5		1.34	
VIT_01s0011g06330	(Q9SIS3) 65-kDa microtubule-associated protein 6	1.45		
VIT_03s0038g03430	(Q9SVE5) Expansin-like a2		1.34	
VIT_03s0063g01150	(Q39224) Protein senescence-related gene 1 (srg1)		2.62	
VIT_03s0088g00400	(Q8LED1) Tubulin alpha-6 chain	1.30	1.74	
VIT_05s0077g01720	(F6H6V3) Lipase SAG101 (Senescence-Associated Gene 101)		–1.60	–1.62
VIT_09s0002g05240	(Q9C968) Cyclin-a2-4	–1.25		
VIT_14s0066g01810	(F6HV24) lipase SAG101 (Senescence-Associated Gene 101)	1.77	–1.54	
VIT_18s0001g08250	(Q6VAF9) Tubulin alpha-4 chain	1.12		
VIT_18s0001g09920	(P42753) Cyclin-d3	–2.03		

Many genes typically related to defence reactions were down-regulated (e.g. thaumatins, chitinases, patatins, pathogenesis-related proteins, the NBS-LRR class of disease resistance proteins, EDS, β1–3 glucanase). Signal transduction was strongly down-regulated; ~50 genes encoding protein kinases were repressed. Transcripts linked to ethylene (such as many *ERF* genes, e.g. VIT_07s0031g00710), cytokinins, gibberellins (gibberellin 20 oxidase 2, VIT_18s0001g01390), abscisic acid [9-*cis*-epoxycarotenoid dioxygenase (*NCED*, VIT_02s0087g00930], and jasmonate (12-oxophytodienoate reductase 2, VIT_18s0041g02270) biosynthetic pathways were activated, while other genes linked to auxin signalling were repressed. In the secondary metabolism category, genes for terpene, flavonol, and lignin biosynthesis were up-regulated, although several transcripts encoding phenylalanine ammonia-lyase (*PAL*, VIT_16s0039g01300) were repressed.

Global gene expression changes in GRSPaV-infected berries

In infected berries at véraison, a limited number of genes were modulated, with a general down-regulation of the main functional categories (Fig. 4; Supplementary Table S2 at *JXB* online).

The functional class of genes related to responses to stress and disease showed the highest number of modulated genes. Surprisingly, 93% of them, such as several *HSP* genes, *PR1*, and the *β1–3 glucanase* gene, were down-regulated. In addition, some genes linked to senescence (*SAG101*, VIT_05s0077g01720), ROS detoxification [peroxidase (*POX*), VIT_06s0004g01180 and glutathione *S*-transferase (*GST*), VIT_16s0039g01070], as well as ethylene and jasmonate signalling, were down-regulated. Interestingly, the up-regulation of *Argonaute 2* (*AGO2*, VIT_10s0042g01180), a gene involved in RNA silencing processes, and the down-regulation of the *HT3* gene (VIT_05s0020g03140), which encodes a hexose transporter in the berry during ripening, were detected.

Validation of microarray data by qRT-PCR

Expression changes in 42 genes, selected among the most interesting ones from microarray experiments, were quantified in leaf, petiole, and berry samples by qRT-PCR. The results were calculated as expression ratios (relative quantity, RQ) between GRSPaV-infected and uninfected organs. Four reference genes (*GAPDH*, *EF1-α*, *Act*, and *Ubi*) were analysed using the geNorm algorithm to evaluate their expression stability in GRSPaV-infected and GRSPaV-free samples, and ranked according to their expression stability measure M (Vandesompele *et al*., 2002). *Act* and *Ubi* were shown to have the lowest M values, indicating that these two genes showed high expression stability in all samples (Supplementary Fig. S2 at *JXB* online). Despite the modulation of several genes involved in cytoskeleton formation in both petiole and leaf samples, the *Act* gene used as a housekeeping gene was not influenced by GRSPaV and was used with *Ubi* for qRT-PCR normalization.

The main trends resulting from the microarray analyses were confirmed for all the transcripts analysed by qRT-PCR. The correlation between expression values obtained by qRT-PCR and microarray was good (R^2=0.79) and highly significant ($P < 0.01$), as attested to by the linear regression analysis performed (Supplementary Fig. S3 at *JXB* online).

Gene expression changes monitored in GRSPaV-infected grapevines at different phenological stages

Molecular responses to GRSPaV infection in grapevine were also analysed in 2011. Among the 42 significantly modulated genes validated by qRT-PCR, 26 genes were selected and their expression was quantified by qRT-PCR at five (four for berry) different developmental stages. Results obtained from 2010 and 2011 véraison (E-L35) qRT-PCR experiments were compared, in order to look for any differences in gene expression regulation between the two years. As no significant changes were observed, it was concluded that the gene expression trends

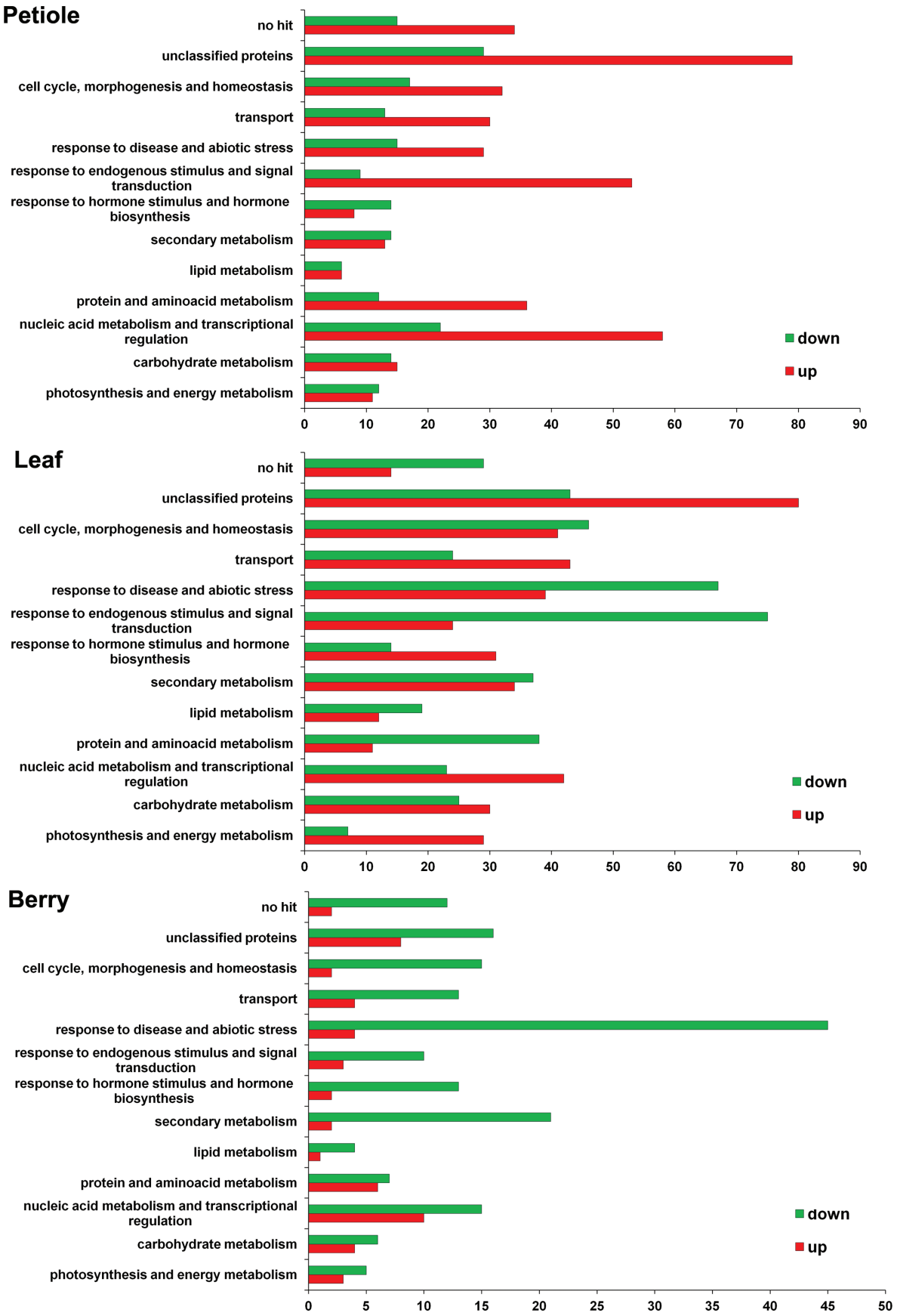

Fig. 4. Functional distribution of grapevine transcripts significantly induced and repressed in GRSPaV-infected petiole, leaf, and berry samples at véraison in 2010. Bars represent the number of transcripts down-regulated (green) or up-regulated (red) within each functional category.

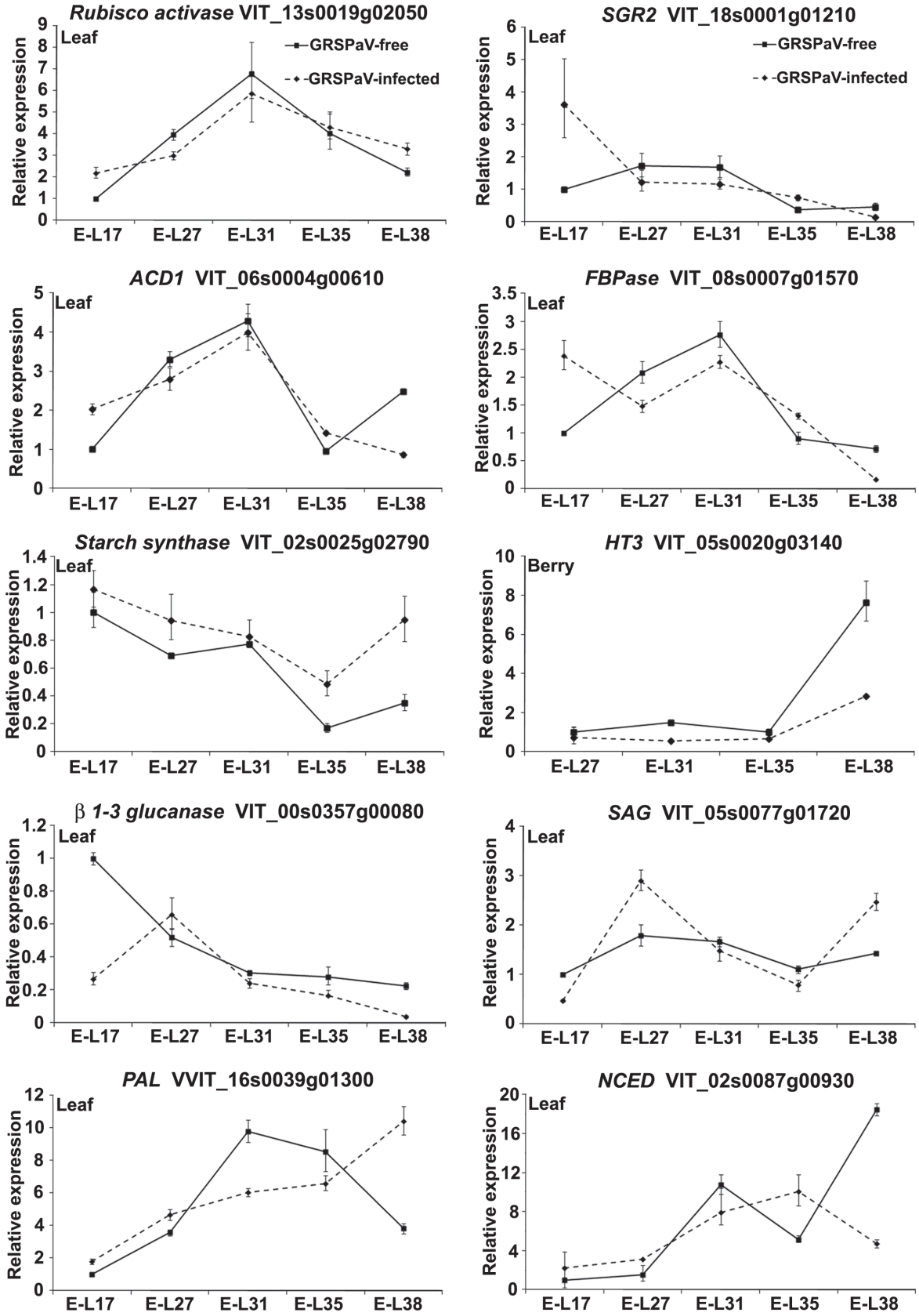

Fig. 5. Relative expression level of *Rubisco activase*, senescence-inducible chloroplast stay-green protein 2 (*SGR2*), accelerated cell death 1 (*ACD1*), fructose 1,6-bisphosphatase (*FBPase*), starch synthase, hexose transporter 3 (*HT3*), *β1–3 glucanase*, senescence-associated gene (*SAG*), phenylalanine ammonia-lyase (*PAL*), and 9-*cis*-epoxycarotenoid dioxygenase (*NCED*) in GRSPaV-free and infected 'Bosco' leaf or berry samples as determined by qRT-PCR. Samples were collected at five developmental stages (four for berries) in 2011. Transcript names refer to the gene ID numbers from the NimbleGen microarray 090818 Vitis exp HX12. qRT-PCR signals were normalized to *Act* and *UBI* transcripts. Data are presented as the mean ±SE of biological and technical replicates.

obtained at véraison in 2010 were confirmed at véraison in 2011 (Supplementary Table S4 at *JXB* online).

Four key genes involved in photosynthesis and chlorophyll degradation [*Rubisco activase*, light-harvesting complex (*LHCII*), VIT_19s0014g00160, *SGR2*, and accelerated cell death 1 (*ACD1*), VIT_06s0004g00610] showed similar trends of expression in 2011. In infected leaves in comparison with GRSPaV-free organs, a strong up-regulation of these genes was observed at the beginning of the season (E-L17, 11 May 2011) (Fig. 5; Supplementary Fig. S4 at *JXB* online). Likewise, the chloroplastic *FBPase*, *GAPDH*, and *FBA* had at least 2-fold overexpression at the beginning of the season (E-L17) compared with GRSPaV-free leaves, while their expression collapsed in infected tissues at harvest (Fig. 5; a Supplementary Fig. S4). In uninfected plants, the expression of *FBPase* and *GAPDH chl* underwent a reduction of ~20% between the beginning (E-L17) and the end (E-L38) of the season, whereas in infected grapevines, this reduction was more significant (~90%). In addition, the expression of these genes was well correlated ($0.80 < R^2 < 0.88$) with the GRSPaV concentration quantified in leaves (Supplementary Fig. S5).

The *starch synthase* gene was generally up-regulated in infected leaves compared with GRSPaV-free organs, while the hexose transporter gene *HT3* was down-regulated, in particular at the E-L38 stage: the transcript levels were 60% lower than in GRSPaV-free berries (Fig. 5).

The *β1–3 glucanase* gene was down-regulated in GRSPaV-infected leaves, in comparison with uninfected organs, at the E-L17 stage and at the end of the season (Fig. 5). In addition, the gene expression level showed a good correlation (R^2=0.91) with GRSPaV concentration at all the different stages analysed (Supplementary Fig. S6 at *JXB* online). In GRSPaV-free berries, the expression trend of *β1–3 glucanase* was strongly increased at véraison and harvest, while in infected berries the increase of *β1–3 glucanase* at the end of the season was less evident: the transcripts were at least 3-fold underexpressed compared with GRSPaV-free organs (Supplementary Fig. S4).

Variable expression during the season was observed for genes involved in secondary metabolism [*PAL*; chalcone synthase (*CHS*), VIT_05s0136g00260; *MybPA1*, VIT_15s0046g00170; *MybA3*, VIT_02s0033g00450; and *NCED*], and for those linked to ROS detoxification [catalase (*CAT3*), VIT_18s0122g01320; dehydroascorbate reductase (*DHAR*), VIT_00s0317g00050; and *POX*] (Fig. 5; Supplementary Fig. S7 at *JXB* online). The senescence-associated gene *SAG101* was up-regulated in infected leaves, in particular during the berry setting phase (E-L27).

In infected leaves and berries, at véraison, and in particular at harvest, a strong up-regulation of *AGO2* compared with GRSPaV-free organs was observed. In addition, in uninfected grapevines, at the first three developmental phases analysed, *AGO2* was at least 3-fold overexpressed in petioles and leaves compared with berries (Fig. 6). In all three organs (petioles, leaves, and berries), the expression levels of this gene were very different and seemed to be inversely related to GRSPaV concentrations (Supplementary Fig. S6 at *JXB* online).

Discussion

During two consecutive years, physiological and agronomic performances together with molecular changes occurring in grapevine plants infected by GRSPaV were analysed. In particular, it was shown that infection with this virus, though not symptomatic, induces strong metabolic changes in *V. vinifera* cv 'Bosco', an Italian white grape variety. As reported by Terlizzi *et al.* (2010), the isolate of GRSPaV present in this clone clustered in the GRSPaV-1 lineage (Meng *et al.*, 2006), and its uneven distribution within the organs was observed, both among different phenological phases and between the two years considered. Viral levels were interestingly higher in berries, whereas other grapevine viruses, such as GLRaV-3, are generally more concentrated in leaves (Vega *et al.*, 2011). The specific cellular localization of GRSPaV is still unknown, although its spread occurs in all the plant tissues. It can thus be assumed that viral particles follow phloem flow, especially toward the berry, the most important sink in grapevine. The lower concentration of virus measured in 2011 could be related to differences in climatic conditions between the two years, such as warmer temperatures in May and August 2011, which led to faster growth rates and an early harvest, and a cooler climate in July 2011 (Supplementary Fig. S8 at *JXB* online). These climatic conditions could have also been responsible for the 'year-effect' observed in physiological and agronomic performances of infected grapevines.

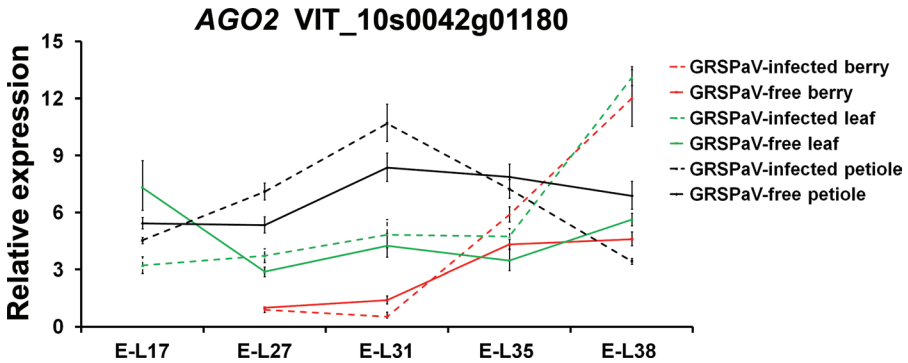

Fig. 6. Relative expression level of *AGO2* in GRSPaV-free and infected 'Bosco' leaf, petiole, and berry samples as determined by qRT-PCR. Samples were collected at five developmental stages (four for berries) in 2011. Transcript name refers to the gene ID number from the NimbleGen microarray 090818 Vitis exp HX12. qRT-PCR signals were normalized to *Act* and *UBI* transcripts. Data are presented as the mean ±SE of biological and technical replicates.

The GRSPaV-free grapevines showed an overall moderate improvement in yield associated with better leaf physiological efficiency. However, the decrease in physiological performance induced by GRSPaV infection was less relevant than what has been observed in other grapevine–virus combinations. For instance, in GRSPaV-infected plants P_n decreased by ~15%, while it is generally reduced by 30% in 'Dolcetto' grapevines infected by GLRaV-3 (Mannini *et al*., 2012), 45% in 'Malvasia' infected by GLRaV and GFLV (Sampol *et al*., 2003), and up to 60% in 'Nebbiolo' infected by GLRaV-3 and GVA (Guidoni *et al*., 1997). Since the P_n data did not seem in agreement with the leaf chlorophyll content measured (in particular in 2011), it is conceivable that infection of grapevines impairs photosynthesis by lowering their carboxylation capacity and mesophyll conductance to CO_2, as has previously been reported by Sampol *et al*. (2003).

Transcriptomic changes in GRSPaV-infected grapevines

The molecular changes induced by GRSPaV in grapevine were initially investigated at 2010 véraison by microarray analysis. Since this virus does not induce macroscopic alterations in *V. vinifera*, véraison was chosen as the best time for sampling because only at the end of the season was observed a moderate decrease of photosynthetic efficiency in infected plants. However, a variation in gene expression among phenological phases was recorded in 2011. The 26 target genes analysed showed variable regulation particularly at the beginning of the season (E-L17, 11 May 2011), corresponding to higher virus accumulation, and at harvest (E-L38, 25 August 2011), when senescence begins parallel to several metabolic changes triggered by GRSPaV. The discussion focuses essentially on microarray data at véraison. Anyway, it is conceivable that in other phenological phases the grapevine response to this virus could be different for some classes of genes, and further investigations are necessary to provide a complete overview of the interactions between GRSPaV and *V. vinifera*.

Photosynthesis and carbohydrate metabolism in GRSPaV-infected grapevines

The metabolic alterations induced by GRSPaV in infected leaves at véraison caused a reduction in P_n in the absence of environmental limitation; thus, the infected grapevine attempted to increase P_n rates by inducing genes involved in photosynthesis and CO_2 fixation. Rubisco activase is a key regulator of photosynthesis and its up-regulation typically enhances photosynthetic efficiency by directly increasing the amount of Rubisco activated for CO_2 fixation (Parry *et al*., 2003). The increased expression of some genes linked to the Calvin cycle, such as chloroplastic *GAPDH*, *FBA*, and in particular *FBPase*, could probably be interpreted as a mechanism to restore ribulose-1,5-bisphosphate (RuBP) upon stress conditions, thus further favouring the initial activity of Rubisco (Tamoi *et al*., 2006). However, the up-regulation of these genes was not sufficient to drive an overall increase in P_n in infected plants. Evidence for similar responses has previously been reported by Baebler *et al*. (2009), who showed a transient increase in photosynthesis-related gene expression immediately after *Potato virus Y* (PVY) inoculation in potato. Interestingly, in young infected leaves (E-L17, 11 May 2011), the genes involved in the Calvin cycle were strongly up-regulated, probably to support viral replication and spread throughout the newly formed organs. In addition, both *GAPDH* isoforms (cytosolic and chloroplastic) analysed in infected leaves showed highly variable expression during some developmental stages. Therefore, in the presence of GRSPaV, this gene should not be used as a housekeeping gene for qRT-PCR experiments (Supplementary Fig. S2 at *JXB* online).

Virus infections have a large stimulatory effect on respiration rates and efficiency of the oxidative pentose phosphate pathway, glycolysis, and the Krebs cycle (Técsi *et al*., 1996; Whitham *et al*., 2003; Espinoza *et al*., 2007*a*; Babu *et al*., 2008). These alterations are frequently associated with the presence of disease symptoms, such as chlorosis. In the leaves of GRSPaV-infected grapevines, the genes involved in all these pathways were down-regulated or not modulated at véraison. The lack of visible symptoms in GRSPaV-infected grapevines could be related to a decrease in primary metabolism.

The expression of *SGR2* and *ACD1* seemed strictly related to chlorophyll turnover in grapevines, probably due to the lack of chlorotic symptoms in infected leaves. *SGR* genes encode members of a family of chloroplast-located proteins, the activity of which is considered to be a prerequisite for both chlorophyll and apoprotein degradation (Hörtensteiner and Kräutler, 2011). Chlorophyll degradation causes the production of extremely phytotoxic light-absorbing chlorophyll breakdown products (porphyrin compounds), which precipitate plant cell death (PCD). *ACD* may control these products: transgenic *Arabidopsis* plants expressing high levels of *ACD* show increased tolerance to infection by *Pseudomonas syringae*, with a reduction in disease symptoms, without affecting the growth of bacteria (Mach *et al*., 2001). It is suggested that, in GRSPaV-infected grapevines, the activation of *ACD1* could hinder the effects of *SGR2* by reducing the PCD and contributing to the absence of chlorotic symptoms in infected leaves.

GRSPaV infection down-regulates the transcription of defence-related genes in grapevine

The down-regulation of many genes involved in the defence response was another surprising result observed in grapevines infected by GRSPaV. Among these genes, the focus was on *β1–3 glucanase* in particular. Higher expression of *β1–3 glucanase* was measured by global gene expression analysis in several virus-infected plants (Whitham *et al*., 2003; Espinoza *et al*., 2007*a*; Ascencio-Ibanez *et al*., 2008; Babu *et al*., 2008; Baebler *et al*., 2009), whereas a down-regulation was observed here in both leaf and berry samples, corresponding to high levels of GRSPaV. In the past, Beffa and Meins (1996) demonstrated that tobacco mutants deficient in the *β1–3 glucanase* gene showed a huge reduction in *Tobacco mosaic virus* (TMV) disease symptoms, suggesting that this decreased susceptibility to the virus was a consequence of the increased deposition of callose. In grapevine infected by GRSPaV, the downregulation of *β1–3 glucanase* could be linked to the absence of macroscopic symptoms.

In GRSPaV-infected tissues (in particular in berries), increased expression of *AGO2* was found. Recent studies have demonstrated

that AGO2 has an antiviral role in *Arabidopsis* against *Turnip crinkle virus* (TCV), *Cucumber mosaic virus* (CMV) (Harvey *et al*., 2011; Wang *et al*., 2011), and *Potato virus X* (PVX) (Jaubert *et al*., 2011), and in *Nicotiana benthamiana* against *Tomato bushy stunt virus* (TBSV) (Scholthof *et al*., 2011). To date, no study is available on the role of AGO proteins in grape antiviral silencing. Nevertheless, the organs with basal high *AGO2* expression (petioles and leaves) had limited GRSPaV concentrations compared with young berries. According to Harvey *et al*. (2011), who found that the loss of *AGO2* in *Arabidopsis* mutants had a drastic effect on TCV and CMV symptoms, with a limited effect on viral accumulation, similar reactions in GRSPaV-infected grapevines can be hypothesized. These observations may represent a starting point for future studies aiming to understand the function of AGO2 in grapevine.

Overlap between the response to GRSPaV and abiotic stresses

Some effects observed in plants infected by viruses are linked to more general responses against several stresses and to metabolic changes occurring at specific plant developmental stages. In grapevines infected by GLRaV-3, an overlap between leaf senescence and plant responses to the virus has already been demonstrated (Espinoza *et al*., 2007*b*). This overlapping response was also found in GRSPaV-infected grapevines, although this association was less clear, in particular in infected leaf and berry tissues, where some genes linked to senescence were repressed. The transcripts of *SAG101*, which plays an important role in senescence processes, in the present 2011 time course analysis increased in the leaves and petioles of infected plants corresponding to the time of berry setting (E-L27, 14 June 2011). In addition, in this phase, *β1–3 glucanase* increased, while *CYCD3;1* and the Calvin cycle genes (chloroplastic *FBPase*, *GAPDH*, and *FBA*) decreased (Fig. 5; Supplementary Fig. S4 at *JXB* online). It is hypothesized that these responses could be related to the climatic conditions occurring in the vineyard at the specific moment when samples were collected for the E-L27 stage. During the day of explant collection (14 June 2011), there was a reduction in temperature associated with light rain, and the same happened on the previous 10 d (Supplementary Fig. S8). These slightly less favourable environmental conditions could have induced the expression of some senescence genes in infected plants and at the same time decreased the expression of genes linked to the cell cycle and CO_2 fixation. Thus, GRSPaV-infected grapevines seem to be more sensitive to environmental changes than uninfected plants, where no significant variation was noticed.

In GRSPaV-infected grapevines, in addition to a partial overlap with senescence, a correlation between responses to water deficiency and salinity stresses was observed. Cramer *et al*. (2007) analysed transcriptomic changes in grapevines subjected to a gradual application of both these abiotic stresses, and for some of these genes (i.e. *Rubisco activase*, *FBA*, photosystem II reaction centre, *CAT*, nitrate and sulphate transporters, aquaporins, NAC transcription factor, gibberellin oxidase, *NCED*, *ACO*, and 12-oxophytodienoate reductase 2) the same modulation was observed in the plants infected by GRSPaV. For the first time in woody plants, to our knowledge, a significant overlap in cellular responses between abiotic stresses, such as water deficiency and salinity, and viral attack has been shown.

Conclusion

The differences in responses to infection observed between several systemic viruses and GRSPaV could be related to a form of adaptation and co-evolution between grapevine and the latter virus, which has been hypothesized to have co-existed with grapevine for a long period of time (Meng *et al*., 2006). Agudelo-Romero *et al*. (2008), in an interesting evolutionary experiment on *Tobacco etch virus* (TEV) in *Arabidopsis*, showed that the evolved virus triggers a different plant transcriptomic pattern compared with ancestral TEV. In particular, genes involved in stress and pathogen responses are not activated in the presence of the evolved virus, suggesting that natural selection has favoured viral strategies to evade host defences. Grapevine is a vegetatively propagated species that, once infected with GRSPaV, remains infected throughout its lifetime, and the virus is transmitted to vegetative progeny. The long co-existence of grapevine and GRSPaV and the absence of a biological vector, associated with frequent errors in genome replication induced by the lack of proofreading activity in viral RdRp, may have resulted in the evolution of less severe viral infections with slight alterations in the host genome.

It would be interesting to verify the molecular responses induced by GRSPaV in other symptomatic *Vitis* spp. and, considering the high variability of the GRSPaV population, the effects of other strains in *V. vinifera*. These observations should be carefully considered in future programmes of clonal selection.

Supplementary data

Supplementary data are available at JXB online.

Figure S1. Physiological parameters analysed in 2011 in GRSPaV-free and GRSPaV-infected leaves of grapevine.

Figure S2. Gene expression stability of reference genes as calculated by geNorm.

Figure S3. Correlation between expression changes quantified by qRT-PCR and microarray in GRSPaV-infected leaves, petioles, and berries.

Figure S4. Relative expression level of LHCII, ACD1, CYCD3;1, AGPase, FBA, GAPDH chl, GAPDH cyt, and β1–3 glucanase in GRSPaV-free and infected leaves, petioles, or berries determined by qRT-PCR during five developmental stages in 2011.

Figure S5. Correlation between relative expression levels of FBPase, FBA, GAPDH chl, SGR2, ACD1, and CYCD3;1, and GRSPaV concentrations.

Figure S6. Correlation between relative expression levels of AGO2, β1–3 glucanase, HT3, and CAT3, and GRSPaV concentrations.

Figure S7. Relative expression level of DHAR, POX, CAT3, SAG, CHS, MYBPA1, MYBA3, and ACO in GRSPaV-free and infected leaves, petioles, or berries determined by qRT-PCR during five developmental stages in 2011.

Figure S8. Daily mean temperature and rainfall during 2010 and 2011 ripening seasons in Albenga (Liguria), North-West Italy.

Table S1. Summary of oligonucleotides used in this study.

Table S2. Complete list of genes with significant expression differences in the GRSPaV-infected versus GRSPaV-free plants at the petiole, leaf, and berry levels.

Table S3. Expression values of 42 genes chosen for microarray validation and analysed by qRT-PCR at véraison in 2010.

Table S4. Expression values of 26 genes analysed by qRT-PCR at véraison in 2010 and 2011.

Acknowledgements

This research was partially funded by Regione Liguria. The authors are grateful to Ivana Gribaudo for critical reading of the manuscript, to Walter Chitarra for the fruitful discussion on physiological performances of virus-infected grapevines, and to Marco Incarbone for English manuscript editing.

References

Agudelo-Romero P, Carbonell P, Pérez-Amador MA, Elena SF. 2008. Virus adaptation by manipulation of host's gene expression. *PLoS ONE* **3,** e2397.

Ascencio-Ibáñez JT, Sozzani R, Lee T-J, Chu T-M, Wolfinger RD, Cella R, Hanley–Bowdoin L. 2008. Global analysis of *Arabidopsis* gene expression uncovers a complex array of changes impacting pathogen response and cell cycle during geminivirus infection. *Plant Physiology* **148,** 436–454.

Babu M, Griffiths JS, Huang TS, Wang A. 2008. Altered gene expression changes in *Arabidopsis* leaf tissues and protoplasts in response to *Plum pox virus* infection. *BMC Genomics* **9,** 325.

Baebler Š, Krečič–Stres H, Rotter A, *et al.* 2009**.** PVY^{NTN} elicits a diverse gene expression response in different potato genotypes in the first 12 h after inoculation. *Molecular Plant Pathology* **10,** 263–275.

Beffa R, Meins F. 1996. Pathogenesis-related functions of plant beta-1, 3-glucanases investigated by antisense transformation—a review. *Gene* **179,** 97–103.

Bouyahia H, Boscia D, Savino V, La Notte P, Pirolo C, Castellano MA, Minafra A, Martelli GP. 2005. *Grapevine rupestris stem pitting-associated virus* is linked with grapevine vein necrosis. *Vitis* **44,** 133–137.

Coombe BG. 1995. Adoption of a system for identifying grapevine growth stages. *Australian Journal of Grape and Wine Research* **1,** 100–110.

Cramer GR, Ergul A, Grimplet J, *et al.* 2007. Water and salinity stress in grapevines: early and late changes in transcript and metabolite profiles. *Functional and Integrative Genomics* **7,** 111–134.

Espinoza C, Medina C, Somerville S, Arce-Johnson P. 2007*b*. Senescence-associated genes induced during compatible viral interactions with grapevine and Arabidopsis. *Journal of Experimental Botany* **58,** 3197–3212.

Espinoza C, Vega A, Medina C, Schlauch K, Cramer G, Arce-Johnson P. 2007*a*. Gene expression associated with compatible viral diseases in grapevine cultivars. *Functional and Integrative Genomics* **7,** 95–110.

Eynard I, Gay G, Arlunno A, Bovio M. 1978. Germogliamento della vite e gelate primaverili. *Atti dell'Accademia Italiana della Vite e del Vino* **30,** 68–86.

Gambino G, Gribaudo I. 2006. Simultaneous detection of nine grapevine viruses by multiplex RT-PCR with coamplification of a plant RNA internal control. *Phytopathology* **96,** 1223–1229.

Gambino G, Minuto M, Boccacci P, Perrone I, Vallania R, Gribaudo I. 2011. Characterization of expression dynamics of WOX homeodomain transcription factors during somatic embryogenesis in *Vitis vinifera*. *Journal of Experimental Botany* **62,** 1089–1101.

Gambino G, Perrone I, Gribaudo I. 2008. A rapid and effective method for RNA extraction from different tissues of grapevine and other woody plants. *Phytochemical Analysis* **19,** 520–525.

Gribaudo I, Gambino G, Cuozzo D, Mannini F. 2006. Attemps to eliminate *Grapevine rupestris stem pitting-associated virus* from grapevine clones. *Journal of Plant Pathology* **88,** 293–298.

Goszczynski DE. 2010. Rugose wood-associated viruses do not appear to be involved in Shiraz (Syrah) decline in South Africa. *Archives of Virology* **155,** 1463–1469.

Guidoni S, Mannini F, Ferrandino A, Argamante N, Di Stefano R. 1997. The effect of grapevine leafroll and rugose wood sanitation on agronomic performance and berry and leaf phenolic content of a Nebbiolo clone (*Vitis vinifera* L.). *American Journal of Enology and Viticulture* **48,** 438–442.

Harvey JJ, Lewsey MG, Patel K, Westwood J, Heimstadt S, Carr JP, Baulcombe DC. 2011. An antiviral defense role of AGO2 in plants. *PLoS ONE* **6,** e14639.

Hörtensteiner S, Kräutler B. 2011. Chlorophyll breakdown in higher plants. *Biochimica et Biophysica Acta* **1807,** 977–988.

Jaubert M, Bhattacharjee S, Mello AF, Perry KL, Moffett P. 2011. ARGONAUTE2 mediates RNA silencing anti-viral defenses against *Potato virus X* in *Arabidopsis*. *Plant Physiology* **156,** 1556–1564.

Komar V, Vigne E, Demangeat G, Lemaire O, Fuchs M. 2010. Comparative performance analysis of virus-infected *Vitis vinifera* cv. Savagnin rose grafted onto three rootstocks. *American Journal of Enology and Viticulture* **61,** 68–73.

Lima MF, Alkowni R, Uyemoto JK, Golino DA, Osman F, Rowhani A. 2006. Molecular analysis of a California strain of *Rupestris stem pitting-associated virus* isolated from declining Syrah grapevines. *Archives of Virology* **151,** 1889–1894.

Mach JM, Castillo AR, Hoogstraten R, Greenberg JT. 2001. The *Arabidopsis* accelerated cell death gene ACD2 encodes red chlorophyll catabolite reductase and suppresses the spread of disease symptoms. *Proceedings of the National Academy of Sciences, USA* **98,** 771–776.

Mannini F, Mollo A, Credi R. 2012. Field performance and wine quality modification in a clone of *Vitis vinifera* cv. Dolcetto after GLRaV-3 elimination. *American Journal of Enology and Viticulture* **63,** 144–147.

Martelli GP. 1993. Rugose wood complex. In: Martelli GP, ed. *Graft-transmissible diseases of grapevines, handbook for detection and diagnosis*. Rome, Italy: Food and Agriculture Organization of the United Nations, 45–54.

Meng B, Gonsalves D. 2003. *Rupestris stem pitting-associated virus* of grapevines: genome structure, genetic diversity, detection, and phylogenetic relationship to other plant viruses. *Current Topics in Virology* **3,** 125–135.

Meng B, Li C,Wang W, Goszczynski D, Gonsalves D. 2005. Complete genome sequences of two new variants of *Grapevine rupestris stem pitting-associated virus* and comparative analyses. *Journal of General Virology* **86,** 1555–1560.

Meng B, Rebelo AR, Fisher E. 2006. Genetic diversity analyses of grapevine *Rupestris stem pitting-associated virus* reveal distinct population structures in scion versus rootstock varieties. *Journal of General Virology* **87,** 1725–1733.

Parry MA, Andralojc PJ, Mitchell RA, Madgwick PJ, Keys AJ. 2003. Manipulation of Rubisco: the amount, activity, function and regulation. *Journal of Experimental Botany* **54,** 1321–1333.

Reid KE, Olsson N, Schlosser J, Peng F, Lund ST. 2006. An optimized grapevine RNA isolation procedure and statistical determination of reference genes for real-time RT-PCR during berry development. *BMC Plant Biology* **6,** 27.

Reynolds AG, Lanterman WS, Wardle DA. 1997. Yield and berry composition of five *Vitis* cultivars as affected by *Rupestris stem pitting virus*. *American Journal of Enology and Viticulture* **48,** 449–458.

Sampol B, Bota J, Riera D, Medrano H, Flexas J. 2003. Analysis of the virus-induced inhibition of photosynthesis in malmsey grapevines. *New Phytologist* **160,** 403–412.

Scholthof HB, Alvarado VY, Vega-Arreguin JC, Ciomperlik J, Odokonyero D, Brosseau C, Jaubert M, Zamora A, Moffett P. 2011. Identification of an ARGONAUTE for antiviral RNA silencing in *Nicotiana benthamiana*. *Plant Physiology* **156,** 1548–1555.

Tamoi M, Nagaoka M, Miyagawa Y, Shigeoka S. 2006. Contribution of fructose-1,6-bisphosphatase and sedoheptulose-1, 7-bisphosphatase to the photosynthetic rate and carbon flow in the Calvin cycle in transgenic plants. *Plant and Cell Physiology* **47,** 380–390.

Técsi LI, Smith AM, Maule AJ, Leegood RC. 1996. A spatial analysis of physiological changes associated with infection of cotyledons of marrow plants with *Cucumber mosaic virus*. *Plant Physiology* **111,** 975–985.

Terlizzi F, Ratti C, Filippini G, Pisi A, Credi R. 2010. Detection and molecular characterization of Italian *Grapevine rupestris stem pitting-associated virus* isolates. *Plant Pathology* **59,** 48–58.

Tusher VG, Tibshirani R, Chu G. 2001. Significance analysis of microarrays applied to the ionizing radiation response. *Proceedings of the National Academy of Sciences, USA* **98,** 5116–5121.

Vandesompele J, De Preter K, Pattyn F, Poppe B, Van Roy N, De Paepe A, Speleman F. 2002. Accurate normalization of real-time quantitative RT-PCR data by geometric averaging of multiple internal control genes. *Genome Biology* **3**, research 0034.

Vega A, Gutiérrez RA, Peña-Neira A, Cramer GR, Arce-Johnson P. 2011. Compatible GLRaV-3 viral infections affect berry ripening decreasing sugar accumulation and anthocyanin biosynthesis in *Vitis vinifera*. *Plant Molecular Biology* **77,** 261–274.

Wang XB, Jovel J, Udomporn P, Wang Y, Wu Q, Li WX, Gasciolli V, Vaucheret H, Ding SW. 2011. The 21-nucleotide, but not 22-nucleotide, viral secondary small interfering RNAs direct potent antiviral defense by two cooperative Argonautes in *Arabidopsis thaliana*. *The Plant Cell* **23,** 1625–1638.

Whitham SA, Quan S, Chang HS, Cooper B, Estes B, Zhu T, Wang X, Hou YM. 2003. Diverse RNA viruses elicit the expression of common sets of genes in susceptible *Arabidopsis thaliana* plants. *The Plant Journal* **33,** 271–283.